Heliyon 8 (2022) e11327

Contents lists available at ScienceDirect

Heliyon

journal homepage: www.cell.com/heliyon

Research article

Application of the singular value and pivoted QR decompositions to reduce experimental efforts in compressor characterization

Andrés Tiseira, Benjamín Pla, Pau Bares, Alexandra Aramburu *

CMT-Motores Térmicos, Universitat Politècnica de València, Camino de Vera s/n, CP46022, Valencia, Spain

HIGHLIGHTS

- A data-driven technique is used for map characterisation.
- Minimisation of the number of operating conditions to be tested is achieved.
- Determination of the optimal location for testing points.
- The method captures the compressor efficiency with high accuracy.
- A trade-off between experimental effort and accuracy is evaluated.

ARTICLE INFO

Keywords:
Centrifugal compressor map
Performance estimation
Optimal placement
Singular value decomposition
QR decomposition

ABSTRACT

Compressor characterization, either by running experiments in a turbocharger test rig or by detailed CFD modelling, can be expensive and time-consuming. In this work, a novel method is proposed which can be used to build a complete compressor map from a reduced number of measured operating points combined with a previously collected database. The methodology is based on the application of the Singular Value Decomposition (SVD) method to acquire the orthonormal bases of a matrix which contains the information of previous compressor observations. These bases are used along with pivoted QR decomposition to obtain the minimum number of measurement points which are required to implement this technique as well as its optimal placement within the map. The reconstruction of two different compressor maps was made to validate the method. The results show a substantially better trade-off between number of testing points and accuracy compared to standard equidistributed sampling.

1. Introduction

The turbocharging system is a widespread technology used by many propulsive systems as it takes advantage of the energy from the exhaust gases to improve fuel consumption which, among other benefits, leads to emissions reduction. Furthermore, this system enables the downsizing strategy in automotive engines, increasing power density while maintaining the same level of performance.

An integral part of the turbocharger is the centrifugal compressor, understanding the performance of this system is an important factor to attain an optimal description of the engine behaviour. Whether for simulation purposes [1, 2] or for generating 1D-models [3, 4, 5], having a thorough knowledge of the compressor's main features is required. These features are mostly captured in the compressor map, which relates the compressor efficiency with the compression ratio, inlet mass and speed. The most common approach to obtain a complete compressor map is by means of extrapolation or interpolation techniques [6, 7, 8] using look-up tables mostly obtained with experimental testing. Numerical methods are also used frequently [9, 10], although they require detailed knowledge of the compressor's geometry. In either case, obtaining complete maps may result in high computational efforts for compressor CFD modelling or high economic cost for experimental testing.

As a result, many research projects have focused on the development of alternative methodologies to estimate the compressor characteristics. Some studies rely on data-driven techniques such as neural networks or regression algorithms which take advantage of an already existing database. Yu et al. [11] use back-propagation neural networks for an

* Corresponding author.
E-mail address: alaror@mot.upv.es (A. Aramburu).

https://doi.org/10.1016/j.heliyon.2022.e11327
Received 24 March 2022; Received in revised form 7 June 2022; Accepted 25 October 2022

Table 1. Compressor database operating ranges.

Parameter	Range	Units
Corrected speed	47.10 - 237.67	[krpm]
Corrected mass flow	0.010 - 0.220	[kg/s]
Pressure ratio	1.04 - 3.91	[–]
Efficiency	0.30 - 0.82	[–]

axial-compressor map prediction. However, in addition to the actual map data, it also requires experimental data provided by the manufacturer. Azzam et al. [12] use artificial neural networks (ANN) to predict the loss coefficient and the pressure ratio as well as some basic geometry parameters from an axial compressor. This technique also requires a large database, which was created based on compressors with different geometries. In both cases, the amount of training data is crucial for learning precision and to an adequate approximation.

As for regression models, partial least squares (PLS) modelling methods have also been used as these require a low sample number and promote robustness [13]. For instance, compressor pressure ratio and efficiency were predicted in [14] using kernel PLS. Peng et al. [15] used three different methods to make a component characteristic reconstruction. Results showed PLS achieves better accuracy compared to traditional methods and back propagation, although the application of PLS depended on the shape of compressor characteristic curves as well as the number of samples available.

In this framework, this paper proposes a data-driven concept to estimate a complete compressor map from a limited number of testing points. The method is based on the study made by Manohar et al. [16] where SVD coupled with QR pivoting is used to optimize the sensor placement for signal reconstruction based on features extracted from a database. SVD can be found in the literature for various uses such as face recognition analysis [17, 18, 19] or for information reconstruction from sparse data in fluid dynamics [20, 21]. Regarding QR, this matrix factorization has proven to be useful in data science applications, particularly for dimension reduction [22, 23].

The scope of this research work is to apply a method, based on SVD and pivoted QR decomposition, capable of estimating a compressor map with a reduced number of samples. Results demonstrate that employing an available experimental database comprised from different compressor types and experimental conditions may reduce testing and computational effort. Besides the introduction, this article is organized as follows: section 2 describes the experimental facilities used for data acquisition. Section 3 is devoted to briefly introduce the main characteristics of SVD and QR as well as to define how these tools are applied. In section 4, the results from the method implementation are presented and the final section concludes with the strengths of the method and its limitations.

2. Experimental setup

Implementation of the SVD-pQR method requires a database, which was generated using the information provided by different compressor maps obtained, over time, in the turbocharger test bench employed in this study. Although, each compressor used in this analysis was implemented in a different ICE engine, all of them are radial flow compressors with similar size characterized by having a similar mass flow range and head coefficient, as well as a similar highest pressure ratio. Table 1 gives the complete operating range covered by the compressors in the database for each of the main features present in a conventional map.

The turbocharger test bench shown in Fig. 1 has been specifically developed to carry out characterization tests on centrifugal compressors and radial turbines. Fig. 2 illustrates a schematic of the installation with two distinct zones. The dotted line shows the power generation zone defined by an engine, a brake, a gearbox and a screw compressor. The engine acts as a gas flow generator, providing energy to the turbocharger to be tested via its exhaust gases. In particular, the enthalpy in the engine exhaust gases driving the turbine is controlled by

Fig. 1. Global view of the experimental facility.

Table 2. Measurement sensors characteristics.

Parameter	Sensor type	Uncertainty
Mass flow	hot mass flow meter	1.1%
Temperature	type K thermocouples	1.52 K
Pressure	piezoresistive transducers	12.5 hPa

acting on the engine speed and load. A screw compressor is used to supercharge the engine, so allowing an additional degree of freedom to control the engine exhaust (so turbine inlet) conditions. The solid line defines the experimental measurement area for the characterization of compressors and turbines. The volume located at the inlet of the turbine laminates the pulsating gas obtaining continuous flow without pulses. Further details on the experimental facility can be found in [24].

The position of the measurement sensors was made according to SAE standards for the characterization of radial compressors on a turbocharger bench [25, 26]. Table 2 presents a summary of the sensors used during the experimental campaigns, the associated uncertainty obtained with a 99.7% level of confidence is also included. Olmeda et al. [27] explain in more detail the quantification of the measurement uncertainty values for the turbocharger test bench.

2.1. Compressor map

A compressor map defines the operating area of a compressor by comparing the main performance metrics: mass flow rate ($\dot{m}$), rotational velocity (ω), pressure ratio (r_c) and isentropic efficiency (η). Fig. 3 shows the compressor maps characterized in this bench that comprise the database. The dots in each map represent the measurement points determined by the mass flow and the rotational speed. These parameters are corrected with the compressor inlet and a reference condition to obtain the corrected mass flow ($\dot{m}_c^*$) and the corrected rotational speed (ω_c^*), as defined by equations (1) and (2).

$$\dot{m}_c^* = \dot{m}\sqrt{\frac{T_1}{T_{ref}}}\frac{P_{ref}}{P_1} \tag{1}$$

$$\omega_c^* = \omega\sqrt{\frac{T_{ref}}{T_1}} \tag{2}$$

where, $P_{ref} = 0.999\ bar$ and $T_{ref} = 293\ K$.

The compressor efficiency surfaces were obtained using a shape-preserving piecewise cubic interpolation. Thus, the performance map presents a relation between the aforementioned parameters: $\eta = f(\dot{m}_c^*, \omega_c^*)$.

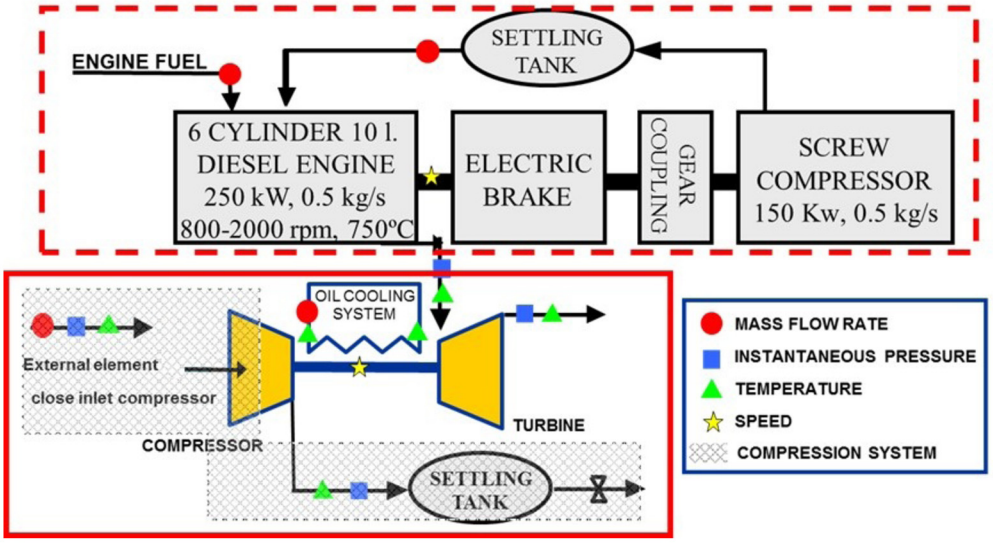

Fig. 2. Experimental set-up.

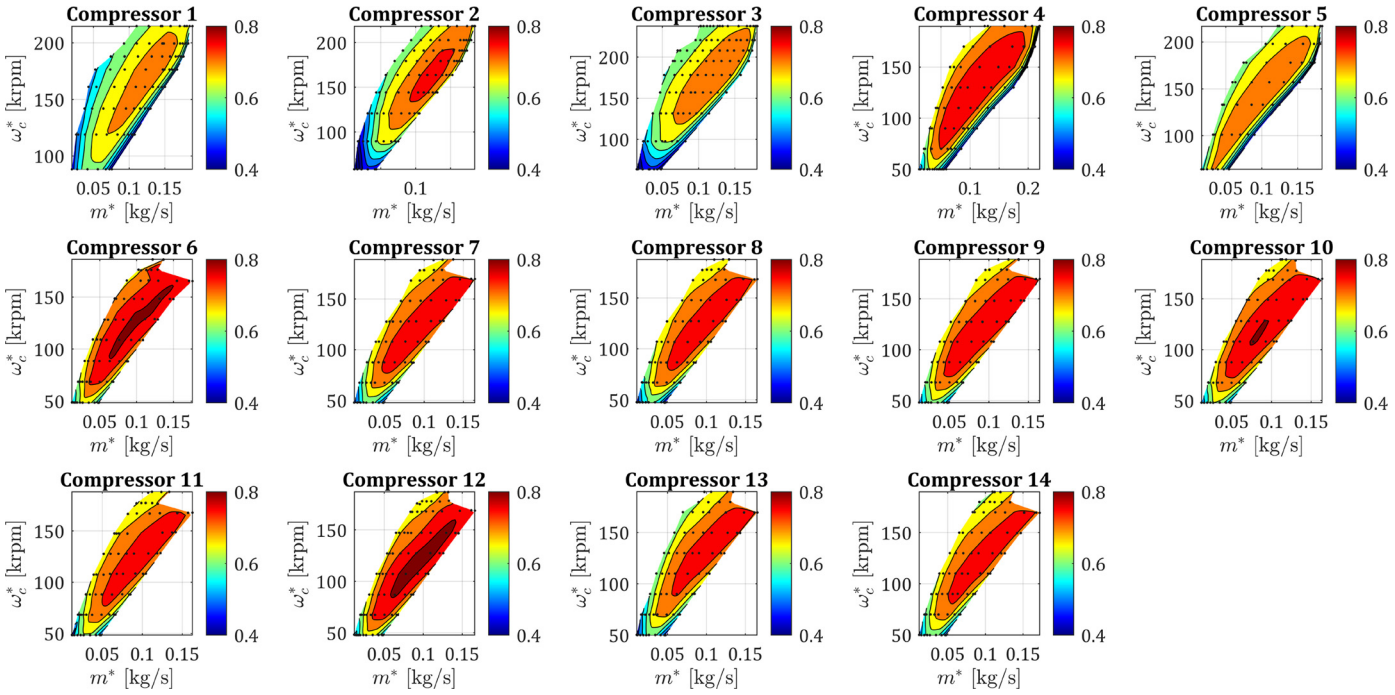

Fig. 3. Complete compressor maps containing the efficiency (η) contour plot versus corrected mas flow ($\dot{m}_c^*$) and corrected velocity (ω_c^*).

3. Methodology

This paper addresses the problem of minimizing the cost of characterising a compressor with a specified level of accuracy. In addition to being ambitious, the above statement is a vague formulation of the problem. On the one hand, it is difficult to properly define a cost in a system with so many factors (facility cost, energy cost, operating cost, post-processing, etc). On the other hand, the level of accuracy cannot be verified a priori, without carrying out validation tests. For this reason, this paper will address the complementary problem of: given a maximum number of points to be tested, place them on the compressor operation map in such a way that the expected error, according to a database, is minimised. Repeating this process with different maximum number of points, a trade-off between experimental effort and accuracy can be estimated. To accomplish this, the following considerations are taken into account:

- The original problem objective (i.e. cost minimization) is relaxed to minimise the number of operating conditions to be tested. This is equivalent to the assumption of a constant operating cost, independent on the tested conditions and that the transition between points is negligible. A discussion on the optimization of the testing order may be found in [28].
- The compressor characterization is, in this paper, represented by the compressor map, i.e. a relation between compressor flow, pressure ratio, speed and efficiency.
- The specified level of accuracy cannot be assured beforehand. Instead, the testing points will be placed to optimally reconstruct (in the sense of minimum mean-square error) the complete compressor map according to a tailored set of modes (or features) extracted from a large set of compressors training data. Note that it is implicitly assumed that the database is somehow representative of the compressor to be characterized.

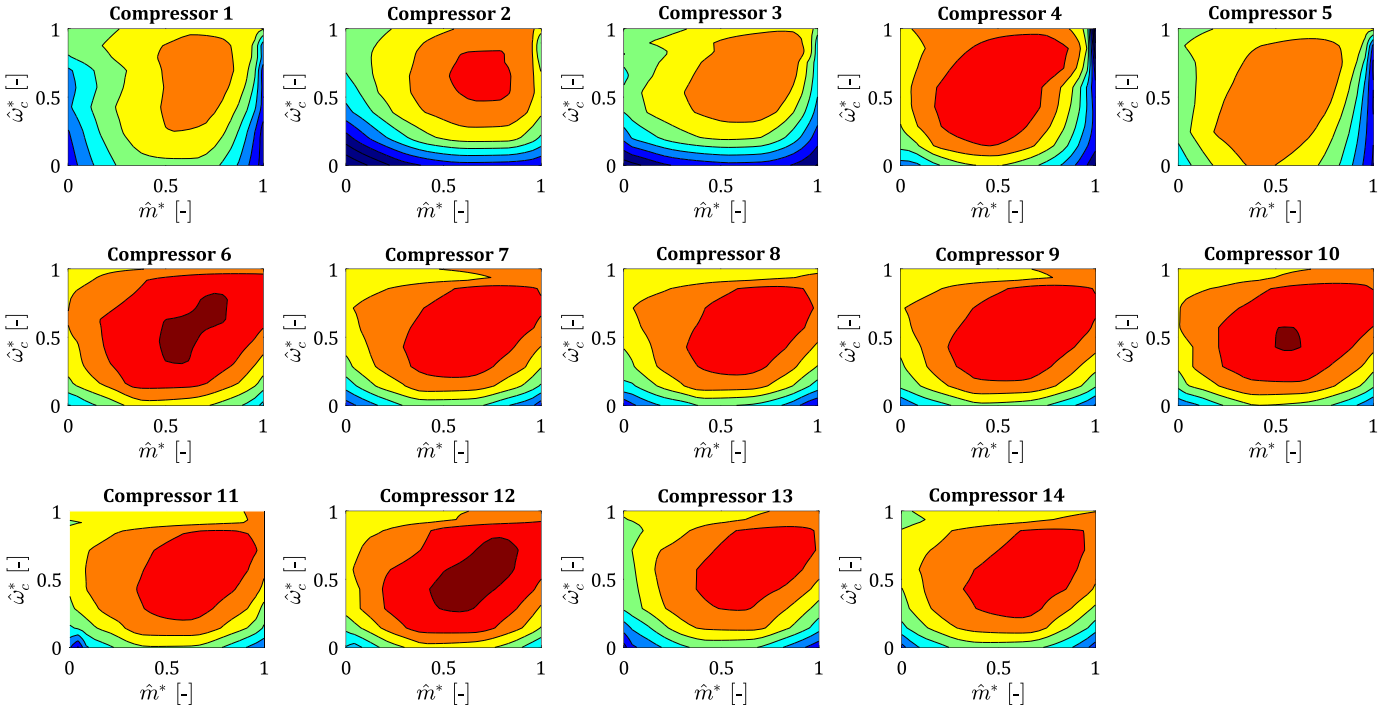

Fig. 4. Compressor normalized database.

In order to achieve the previous objective, three main steps should be followed:

1. Compressor map definition and normalization, i.e. express the relation between compressor variables (mass, compression ratio, speed and flow) in a basis that allows to compare compressors with different features (sizes, geometries, etc)
2. Provided a large data-set with a high dimension (m), obtain a low-dimensional representation ($p \ll m$), aimed to compress the information in a low rank (p) matrix containing the key features of the data-set. To this aim, SVD will be used.
3. Considering the low-rank representation obtained in step 2, choose the best p conditions to reconstruct the complete compressor map. To this aim, pivoted QR decomposition will be used.

The previous three steps are described in the following subsections.

3.1. Compressor map normalization

Before performing the data factorization into its main modes, a database normalization was made as features can have different scaling. This procedure intends to non-dimensionalize the main parameters required to represent the compressor map. SVD depends on the coordinate system in which the data is represented, hence the importance of pre-processing the database.

The map is conventionally presented in a standard form with the efficiency (η) as a function of the pressure ratio and the corrected mass flow. However, for normalization purposes the map will be analysed in an alternative form with the corrected rotational speed instead of the pressure ratio (see Fig. 3), then $\eta = f(\dot{m}_c^*, \omega_c^*)$. For each iso-speed line, normalization was made using the corresponding minimum and maximum $\dot{m}_c^*$, assuming that both increase linearly with ω_c^*. For this procedure, at least the extreme values of the mass flow should be measured; the surge line will define the lower mass flow rate points and the choke line the higher mass flow rate.

The normalized range of both variables, ω_c^* and $\dot{m}_c^*$, lies between 0 and 1 following equations (3) and (4), respectively. The compressor maps after the normalization are shown in Fig. 4.

$$\hat{\omega}_c^* = \frac{\omega_c^* - \omega_{min}^*}{\omega_{max}^* - \omega_{min}^*} \tag{3}$$

$$\hat{m}_c^* = \frac{\dot{m}_c^* - \dot{m}_{min}^*}{\dot{m}_{max}^* - \dot{m}_{min}^*} \tag{4}$$

3.2. Singular value decomposition

Consider a matrix $X \in \mathbb{C}^{n \times m}$ as shown in equation (5).

$$X = \begin{bmatrix} \uparrow & \uparrow & & \uparrow & & \uparrow \\ x_1 & x_2 & \cdots & x_j & \cdots & x_m \\ \downarrow & \downarrow & & \downarrow & & \downarrow \end{bmatrix} \tag{5}$$

X is a collection of m column vectors, where m is the number of species in the database (in this case the amount of compressor maps) and n is the number of points employed to represent each compressor map. The representation consists on a grid of 25 points in the corrected flow axis and 50 points in the corrected speed axis depicting the efficiency value. This grid is reshaped into a column that will be used to generate the X matrix. In this sense, each column x will have $n = 25 \times 50 = 1250$ elements.

Then, the SVD of X performs a factorization into the product of three other matrices as shown in equation (6).

$$X = U \Sigma V^T \tag{6}$$

where $U \in \mathbb{R}^{n \times n}$, $\Sigma \in \mathbb{R}^{n \times m}$ and $V^T \in \mathbb{R}^{m \times m}$.

U and V are unitary and orthogonal matrices hierarchically arranged in terms of their ability to describe the variance in the columns and rows of X respectively. Σ is a diagonal matrix with decreasing, non-negative singular values. In this sense, The SVD is a matrix decomposition method that reduces some real or complex matrix into key features which can be used to make a better analysis or description of the original data.

The diagonal values in the Σ matrix are known as the singular values of the original matrix X. The columns of the U matrix are called the left-singular vectors of X, and the columns of V are called the right-singular vectors of X.

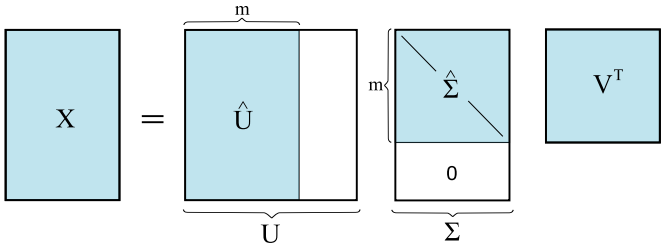

Fig. 5. Reduced SVD scheme.

Usually, there are more measurements than species $n \gg m$. However, as there are only m non-zero singular values, U and Σ can be reduced by selecting the first m columns in U and the first $m \times m$ sub-matrix from Σ to obtain an economic version from the SVD, an schematic representation of the process can be seen in Fig. 5.

This reduced version is still an exact decomposition of the original matrix X, then equation (7) is equivalent to equation (6).

$$X = \hat{U}\hat{\Sigma}V^T = U\Sigma V^T \tag{7}$$

where $\hat{U} \in \mathbb{R}^{n\times m}$, $\hat{\Sigma} \in \mathbb{R}^{m\times m}$ and $V^T \in \mathbb{R}^{m\times m}$.

3.3. Compressor map reconstruction

Once the base matrix $\hat{U}$ for the compressor database was obtained, two subjects must be addressed:

- The first one refers to the number of elements from this base that should be used. A trade-off between precision and time exists, as a large number of elements will ensure a better precision but will be time consuming and can even cause overfitting, considering that the database may have several number of features.
- The other subject refers to the amount and location of the testing points from the new compressor to have the better map estimation. The testing point placement will not be unique, varying from one case to another.

3.3.1. Reduced rank model

To obtain the optimal number of features to use, an SVD truncation was applied. According to the Eckhart-Young theorem [29], given a defined rank $p < m$, the SVD provides the best possible rank-p approximation to matrix X in a least square error sense.

Since both the singular vectors $\hat{U}$ and V are unitary, only the singular values in $\hat{\Sigma}$ represent the weights of the different modes. If most of the information given by X is captured in the first p singular values, then a reduced rank approximation to X only in terms of these dominant values can be made. This rank truncation threshold has to ensure that the signal content is preserved by the SVD, then equation (8) can be used to obtain the number of modes (p) that returns a certain level of representation h.

$$100\% \times \frac{\sum_1^p \sigma_k}{\sum_1^m \sigma_k} \geq h \tag{8}$$

Once the rank of the model is decided, $\hat{U}$ can be resized by using only the first p columns, similar to what has been done for the reduced SVD representation.

3.3.2. Optimal testing points placement

The last topic to be addressed is to find the operating points that need to be measured from the new compressor to obtain an optimal map estimation. Provided that $\hat{U}_{n\times m}$ is a base for the space of all the possible compressor maps, then, a given compressor map (x) can be expressed as:

$$x_{n\times 1} = \hat{U}_{n\times m}\alpha_{m\times 1} \tag{9}$$

with $\alpha \in \mathbb{R}^m$ the coefficients of x in the $\hat{U}$ basis.

Based on the previous subsection, consider using a $\hat{U}$ subset of rank p as a basis, then, $m = p$ in equation (9). In addition, from all the available measurements in x only a limited set $y_{p\times 1}$ was selected. In this sense, one can define a sparse matrix C, whose entrances are zeros or ones, to obtain y by pre-multiplication of vector x:

$$y_{p\times 1} = C_{p\times n}x_{n\times 1} \tag{10}$$

Combining equation (9) and (10), a relation is defined between the location of the optimal points, given by C matrix, and the basis $\hat{U}_{n\times p}$ obtained previously.

$$y_{p\times 1} = C_{p\times n}\hat{U}_{n\times p}\alpha_{p\times 1} \tag{11}$$

As equation (11) can be solved for α, the question arising is the structure of matrix C, which entrances should be zeros and ones, to make the inverse of CU as well-conditioned as possible. To do that, C should be chosen in a way that minimizes the condition number of CU. Considering that the condition number is related to the spectral characteristics of the matrix, a general approximation for the condition matrix minimization is the determinant maximization (that leads to D-Optimal Design of Experiments).

3.3.3. QR decomposition

In this work, instead of using complex Design of Experiments techniques, pivoting QR decomposition is used to obtain the proper matrix C. This method consists on a factorization of an $n \times p$ matrix A into the product of orthonormal (Q) and upper triangular (R) matrices through a column permutation (pivoting) matrix P (see equation (12)), which is mainly used for system equation solving by elimination [30].

$$AP = QR \tag{12}$$

The resulting pivot matrix P orders the elements in the triangular matrix R in decreasing order ($|R_{11}| \geq |R_{22}| \geq \cdots |R_{pp}|$). To do that, the pivoting method is based on maximizing $|R_{ii}|$ at each step of the factorization, so becomes a greedy approximation to the determinant of R [31]. For the case at hand, permutation matrix C, which approximates the best sampling for the p basis modes, can be obtained by performing pivoted QR decomposition [32, 33] over the transpose of singular vector matrix $\hat{U}$.

$$U^T_{n\times p} = QRC \quad \Leftrightarrow U^T_{n\times p}C^T = QR \tag{13}$$

Once the C matrix is defined, the coefficients α can be obtained with an inversion as in equation (14).

$$\alpha_{p\times 1} = (C_{p\times n}\hat{U}_{n\times p})^{-1}y_{p\times 1} \tag{14}$$

At last, the compressor map can be reconstructed with equation (9) considering $m = p$. Fig. 6 depicts a scheme of the steps followed throughout the methodology.

4. Analysis and results

To validate the method, two different compressors were selected randomly (for example purposes compressors 2 and 11 have been extracted). With the complete normalized database, the X' matrix was defined using all the compressors but the one selected for validation. The 2D information from each map, portrayed in the aforementioned grid (see section 3.2), was reshaped into the $m = 13$ columns of X'. The final X matrix was obtained subtracting the mean compressor matrix to the X' matrix, then, the economic SVD was applied over X.

This strategy was implemented for the reconstruction of each of the compressor maps selected. In both cases, at least 6 modes are required to capture more than 90% of the original map, according to the rank evaluation (see Fig. 7). The main modes obtained from this procedure are shown in the lower plot with its corresponding singular value. As

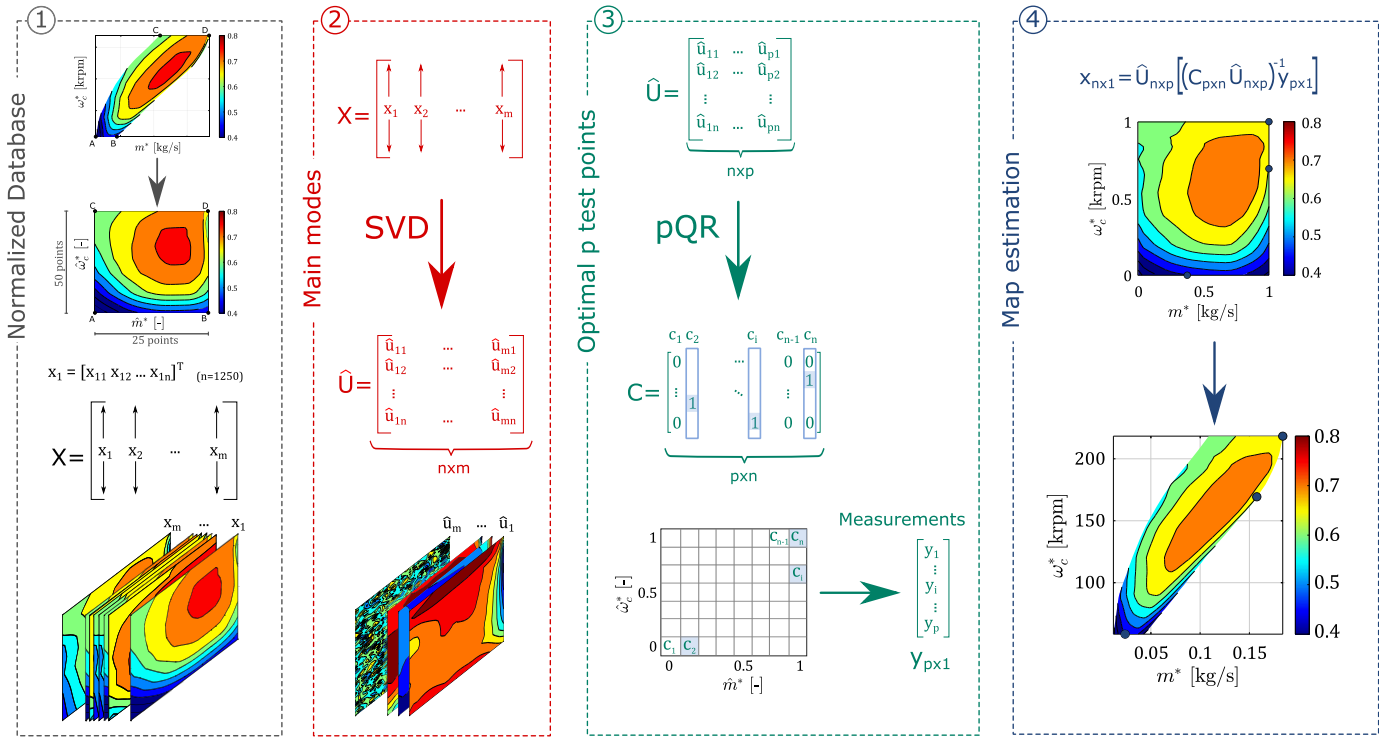

Fig. 6. Model scheme.

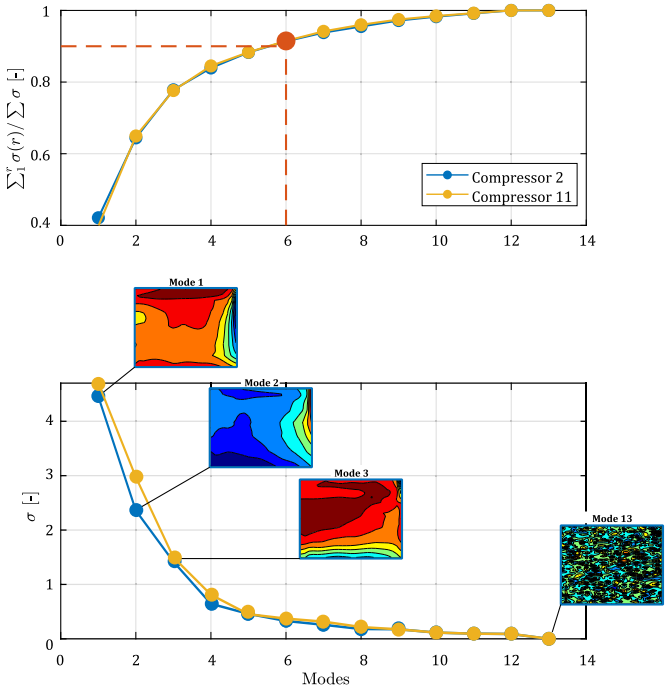

Fig. 7. Upper: SVD rank evaluation for 90% representation. **Lower:** The main modes associated to the first singular values represent most of the original database variations, whereas the last modes present mostly noise.

was mentioned in section 3.3, the first modes are more representative of the original matrix. Information is indeed less significant for higher modes, such as in mode 13 which shows mostly noise. In the case at hand, the method will be applied using from 2 up to 12 modes, to check the method accuracy depending on the number of modes chosen.

The first estimated map corresponds to compressor 2, which was originally obtained by interpolation with 84 measurement points. Fig. 8 (upper plot) shows the reconstructed maps using 2, 10 and 12 testing points. As can be seen in the upper figures, the method is able to capture some general trends. For instance, the region corresponding to the maximum efficiency can be identified, as well as most of the efficiency islands. However, near the surge line some discrepancies can be observed, in fact, the points that present more than a 5% error are mostly located in this area and also along the choke limit. Regarding the number of testing points, the lower plots show an increase of the accuracy as the number of measurements increase. Although beyond 10 points no significant change is observed in the mean absolute error (MAE), the predictability seems to decrease for a large number of testing points. An analysis on the residuals indicates that over-fitting may occur beyond $p = 7$. Fig. 10 displays the residuals standard deviation ($\sigma_{residuals}$) for the case at hand.

The second map estimation was made for compressor 11, which was originally obtained by interpolation with 70 measurements points. Results are presented in Fig. 9, overall, the estimation is accurate for most of the efficiency values. The map is correctly captured showing most of the differences near the boundary areas. In contrast with the previous compressor, this map presents a lower efficiency range which allows an easier detection. It is worth mentioning that despite compressor 11 was taken out of the database, the same compressor with a different inlet remained in the database unlike compressor 2 which did not have any similar one. This will also explain why this compressor was better estimated. As with the previous compressor, the $\sigma_{residuals}$ analysis in Fig. 10 indicates that larger number of testing points are prone to over-fitting. This can be attributed to the fact that the last modes contain more noise.

Finally, a comparison between the SVD-pQR method and progressive testing is made. For progressive testing interpolation was made taking equidistant points from matrix X. Since the result of the progressive testing will depend on the position of the testing points, several combinations have been tested for a given number of tests. The MAE was used to compare the results as shown in Fig. 11. The efficiency of the SVD-QR method is clearly appreciated. For compressor 2 a minimum absolute error of 0.02 is attained using at least 6 testing points, whereas using progressive testing more than 12 points are needed to achieve the

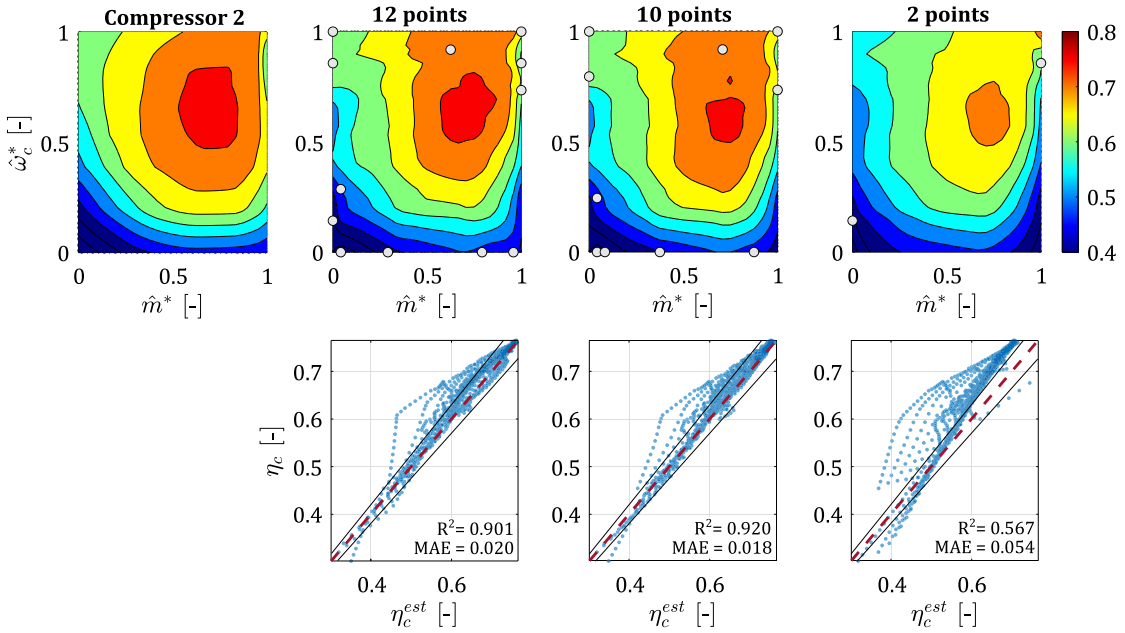

Fig. 8. Upper: Compressor 2 reconstruction for different testing points. **Lower:** Comparison between measured and estimated efficiency values. Black lines represent the ±5% error limit.

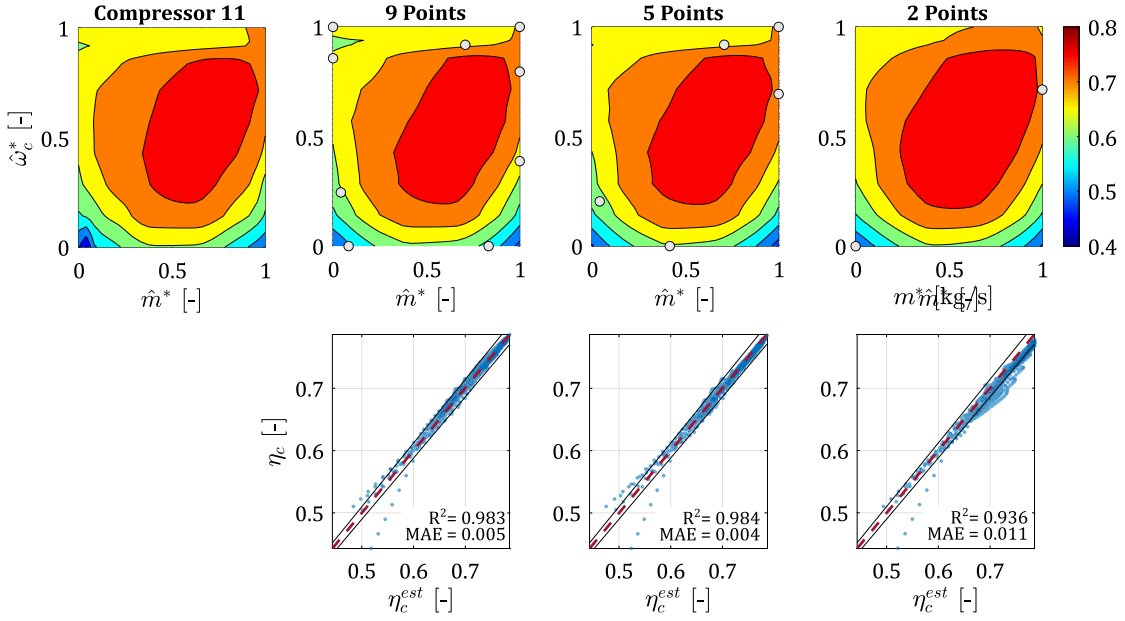

Fig. 9. Upper: Compressor 11 reconstruction for different testing points. **Lower:** Comparison between measured and estimated efficiency values. Black lines represent the ±2% error limit.

same error. As for compressor 11, the same trend is observed; in this case the minimum error was below 0.01 which corresponds with the previous analysis. However, progressive testing seems to have a similar response regardless of the compressor, then, it requires more than 30 testing points to reach a similar relative error.

The point reduction (PR) percentage compared to progressive testing is analysed in Fig. 12. This reduction is measured as described in equation (15), where N_{svd} and N_{pt} refers to the number of points used with the SVD + pQR method and with progressive testing, respectively.

$$PR[\%] = 100\frac{\left|N_{svd} - N_{pt}\right|}{N_{pt}} \tag{15}$$

For comparison purposes, the mean error was obtained for the progressive testing combinations with the same number of points. Results show the effectiveness of the SVD-pQR method to optimally place the measuring points: to attain the same MAE, the method requires over 60% less points compared to progressive testing for both of the compressors estimation. Certainly, the reduction is limited by the number of available test points, as this is related to the level of accuracy that the method is able to reach.

5. Conclusions

In this paper, a new method for estimating compressor maps with reduced testing information was proposed. This method uses SVD and pivoted QR decomposition to reconstruct a compressor map based on a

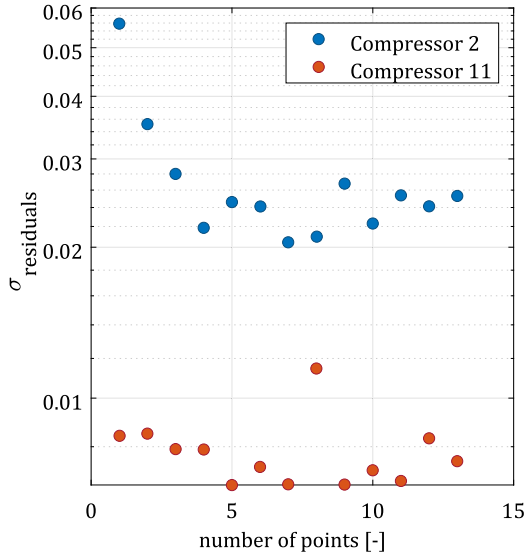

Fig. 10. Residuals standard deviation for both validation tests, shown in logarithmic scale.

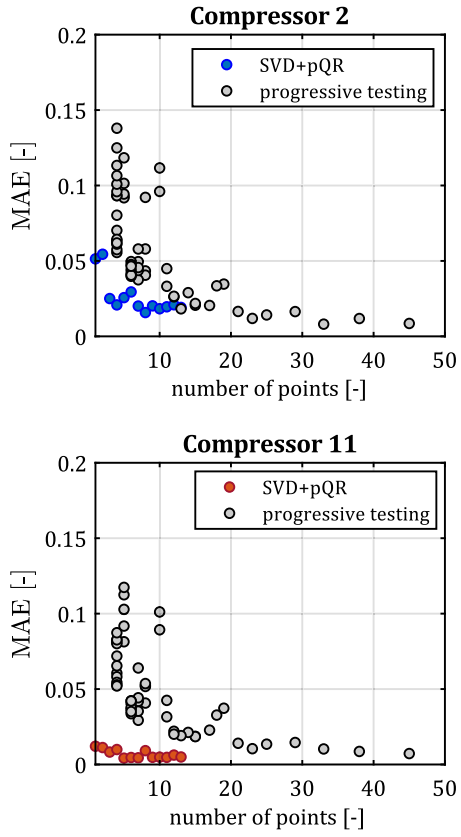

Fig. 11. Estimation error comparison for the SVD-pQR method against progressive testing.

previous database. The importance of this procedure is that it minimizes the compressor estimation error given a reduced number of testing points which is an advantage in terms of time and resources needed.

The method was applied in two different compressors, demonstrating an optimal capability to estimate both maps. In both compressors tested, the mean absolute error represented less than 2% of the efficiency with at least 6 measurement points, while standard progressive testing shows errors above 5% for the same number of points. More importantly, the method was able to capture most of the map information

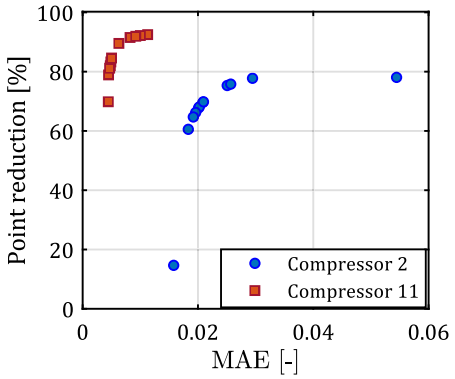

Fig. 12. Point reduction attained with SVD + pQR method comparing with progressive testing method.

using between 6 to 10 points. Results also highlight the importance of assembling a suitable database that is representative of the compressor to be analysed.

Overall, this method can be used to obtain a complete compressor map when some of the information is missing or few experimental operating points are available. It can also be useful in applications with low computational resources where using a high amount of data points may be detrimental.

Declarations

Author contribution statement

Andres Tiseira: Conceived and designed the experiments; Performed the experiments; Contributed reagents, materials, analysis tools or data. **Benjamín Pla:** Analyzed and interpreted the data; Contributed reagents, materials, analysis tools or data. **Pau Bares:** Analyzed and interpreted the data. **Alexandra Aramburu:** Analyzed and interpreted the data; Wrote the paper.

Funding statement

Alexandra Aramburu was supported by Universitat Politècnica de València (FPI-2020-S2-21440).

Data availability statement

The authors do not have permission to share data.

Declaration of interests statement

The authors declare no conflict of interest.

Additional information

No additional information is available for this paper.

References

[1] Jie Li, Yuting Yin, Shuqi Li, Jizhong Zhang, Numerical simulation investigation on centrifugal compressor performance of turbocharger, J. Mech. Sci. Technol. 27 (6) (2013) 1597–1601.

[2] Xiaohan Jia, Bin Zhao, Jianmei Feng, Sulu Zheng, Xueyuan Peng, Numerical simulation and experimental investigation on suction heating of a bog compressor, Appl. Therm. Eng. 108 (2016) 1147–1157.

[3] J. Galindo, F.J. Arnau, A. Tiseira, P. Piqueras, Solution of the turbocompressor boundary condition for one-dimensional gas-dynamic codes, Math. Comput. Model. 52 (7) (2010) 1288–1297.

[4] Calogero Avola, Colin Copeland, Tomasz Duda, Richard Burke, Sam Akehurst, Chris Brace, Review of turbocharger mapping and 1d modelling inaccuracies with specific focus on two-stag systems, Technical report, SAE Technical Paper, 2015.

[5] Pavlos Dimitriou, Richard Burke, Qingning Zhang, Colin Copeland, Harald Stoffels, Electric turbocharging for energy regeneration and increased efficiency at real driving conditions, Appl. Sci. 7 (4) (2017) 350.
[6] P.K. Zachos, I. Aslanidou, V. Pachidis, R. Singh, A sub-idle compressor characteristic generation method with enhanced physical background, J. Eng. Gas Turbines Power 133 (8) (2011).
[7] J. Galindo, A. Tiseira, R. Navarro, D. Tari, H. Tartoussi, S. Guilain, Compressor efficiency extrapolation for 0d-1d engine simulations, Technical report, SAE Technical Paper, 2016.
[8] M. Casey, C. Robinson, A method to estimate the performance map of a centrifugal compressor stage, J. Turbomach. 135 (2) (2013) 021034.
[9] José Galindo, Pablo Fajardo, R. Navarro, L.M. García-Cuevas, Characterization of a radial turbocharger turbine in pulsating flow by means of cfd and its application to engine modeling, Appl. Energy 103 (2013) 116–127.
[10] Enrico Rinaldi, Rene Pecnik, Piero Colonna, Numerical computation of the performance map of a supercritical co2 radial compressor by means of three-dimensional cfd simulations, in: Turbo Expo: Power for Land, Sea, and Air, vol. 45660, American Society of Mechanical Engineers, 2014, V03BT36A017.
[11] Youhong Yu, Lingen Chen, Fengrui Sun, Chih Wu, Neural-network based analysis and prediction of a compressor's characteristic performance map, Appl. Energy 84 (1) (2007) 48–55.
[12] Mark Azzam, Jan-Christoph Haag, Peter Jeschke, Application concept of artificial neural networks for turbomachinery design, Comput. Assist. Methods Eng. Sci. 16 (2) (2017) 143–160.
[13] Xu Li, Chuanlei Yang, Yinyan Wang, Hechun Wang, Xianghuan Zu, Yongrui Sun, Song Hu, Compressor map regression modelling based on partial least squares, R. Soc. Open Sci. 5 (8) (2018).
[14] Fei Chu, Fuli Wang, Xiaogang Wang, Shuning Zhang, Performance modeling of centrifugal compressor using kernel partial least squares, Appl. Therm. Eng. 44 (2012) 90–99.
[15] Shuhong Peng, Bo Sun, Yulong Ying, Keliang Wu, Lei He, Qiang Xu, Accuracy research on the modeling methods of the gas turbine components characteristics, in: Turbo Expo: Power for Land, Sea, and Air, vol. 45653, American Society of Mechanical Engineers, 2014.
[16] K. Manohar, B.W. Brunton, J.N. Kutz, S.L. Brunton, Data-driven sparse sensor placement for reconstruction: demonstrating the benefits of exploiting known patterns, IEEE Control Syst. Mag. 38 (3) (2018) 63–86.
[17] Katerina Fronckova, Pavel Prazak, Antonin Slaby, Singular value decomposition and principal component analysis in face images recognition and fsvdr of faces, in: International Conference on Information Systems Architecture and Technology, Springer, 2018, pp. 105–114.
[18] Jiwen Lu, Yongwei Zhao, Dominant singular value decomposition representation for face recognition, Signal Process. 90 (6) (2010) 2087–2093.
[19] Xuansheng Wang, Zheqi Lin, Zhen Chen, Augmented Lanczos bidiagonalization by small singular value decompositions for face recognition and image compression, Optik 125 (16) (2014) 4411–4416.
[20] Balaji Jayaraman, S.M. Mamun, On data-driven sparse sensing and linear estimation of fluid flows, Sensors 20 (13) (2020).
[21] S.M. Al Mamun, Chen Lu, Balaji Jayaraman, Extreme learning machines as encoders for sparse reconstruction, Fluids 3 (4) (2018).
[22] Jieping Ye, Qi Li, Hui Xiong, H. Park, R. Janardan, V. Kumar, Idr/qr: an incremental dimension reduction algorithm via qr decomposition, IEEE Trans. Knowl. Data Eng. 17 (9) (2005).
[23] Petar Mlinarić, Sara Grundel, Peter Benner, Efficient model order reduction for multi-agent systems using qr decomposition-based clustering, in: 2015 54th IEEE Conference on Decision and Control (CDC), 2015, pp. 4794–4799.
[24] J.M. Lujan, V. Bermudez, J.R. Serrano, C. Cervello, Test bench for turbocharger groups characterization, SAE Technical Papers, 2002.
[25] August SAE J1723. Supercharger Testing Standard, Society of Automotive Engineers, Inc., 1995.
[26] March SAE J1826. Turbocharger Gas Stand Test Code, Society of Automotive Engineers, Inc., 1995.
[27] P. Olmeda, A. Tiseira, V. Dolz, L.M. García-Cuevas, Uncertainties in power computations in a turbocharger test bench, Measurement 59 (2015) 363–371.
[28] Max Johansson, Lars Eriksson, Time optimal turbocharger testing in gas stands with a known map, in: 5th IFAC Conference on Engine and Powertrain Control, Simulation and Modeling, E-CoSM 2018, South Lake Hotel, Changchun, China, September 2018.
[29] Carl Eckart, Gale Young, The approximation of one matrix by another of lower rank, Psychometrika 1 (3) (1936) 211–218.
[30] E. Anderson, Zhaojun Bai, J. Dongarra, Generalized qr factorization and its applications, Linear Algebra Appl. 162 (1992).
[31] H. Engler, The behavior of the qr-factorization algorithm with column pivoting, Appl. Math. Lett. 10 (6) (1997) 7–11.
[32] Gregorio Quintana-Ortí, Xiaobai Sun, Christian H. Bischof, A blas-3 version of the qr factorization with column pivoting, SIAM J. Sci. Comput. 19 (5) (1998) 1486–1494.
[33] Edward Anderson, Zhaojun Bai, Christian Bischof, L. Susan Blackford, James Demmel, Jack Dongarra, Jeremy Du Croz, Anne Greenbaum, Sven Hammarling, Alan McKenney, et al., LAPACK Users' Guide, SIAM, 1999.